Temperature Effect on Supramolecular Hydrogel Gelation Process: A High-Resolution and Fast-Field Cycling NMR Study

Corentin Boulogne, Gaëlle Cogneaux, Paul Hoschtettler, Marie-christine Averlant-Petit, Loïc Stefan, Carole Gardiennet, Sabine Bouguet-Bonnet

Temperature effect on supramolecular hydrogel gelation process: a High Resolution and Fast Field Cycling NMR study.

Corentin Boulogne[1], Gaëlle Cogneaux[1], Paul Hoschtettler[2], Marie-Christine Averlant-Petit[2], Loïc Stefan[2], Carole Gardiennet[1]*, Sabine Bouguet-Bonnet[1]*

[1]CRM2, Université de Lorraine, CNRS, F-54500, Vandœuvre-lès-Nancy, France

[2]LCPM, Université de Lorraine, CNRS, F-54000, Nancy, France

Keywords: FFC ^{1}H-NMR relaxometry, nuclear magnetic resonance dispersion profile, nucleopeptide hydrogel, gelation kinetics

Abstract

Peptide-based supramolecular hydrogels are well known for their biocompatibility and the various range of applications in biotechnologies. The grafting of nucleobases along with the multicomponent approach allows a fine tuning of the hydrogel properties to match new uses. Such adjustments rely on a precise understanding of the material at the atomic level, and Nuclear Magnetic Resonance spectroscopy is a tool of choice for soft matter study. High-Resolution NMR and Fast Field Cycling NMR relaxation can be used to investigate the hydrogel gelation process through the study of the gelator signal and the water dynamical behavior along the gelation time. NMRD profiles can also bring insights into the presence of different water pools and their mobility inside the hydrogel matrix by modeling dispersion curves and extracting correlation times. Measurements were performed at two different temperatures, 295 K and 313 K. Examining the effect of temperature provides insight into the mechanism underlying the transition from solution to gel. This approach highlights not only how an increase in temperature influences the gelation process but also how it affects solvent dynamics within the gelator structure.

1. INTRODUCTION

Peptide-based supramolecular hydrogels are of great interest since few years thanks to their versatility in terms of structures, mechanical properties and type of objects they can form[1–4]. Their biocompatibility, biodegradability and low immunogenicity make this type of gels suitable to many biological and biotechnological applications, such as cell-culture media. Peptide-based hydrogels properties can be tuned by chemical modifications[5–7] such as the introduction of non-natural amino-acids or aromatic moieties, but such modifications remain limited. A solution to such limitation is the grafting of nucleobases in peptide sequences, an emerging way to enhance the versatility of peptide-based hydrogels. Such chemical compounds have great ability to self-assemble thanks to multiple H-bond sites and canonical pairing adenine/thymine (A/T) and cytosine/guanine (C/G)[8,9]. Another possibility is the multicomponent approach. Common in natural biological systems, multicomponent peptide-based hydrogels allow more precision than the monocomponent ones on the control of their mechanical properties, structure morphologies and gelation kinetics by adjusting the ratio between the components. Obviously, multicomponent peptide-based hydrogels remain biocompatible and thus promising for further uses in biotechnological fields.

Multicomponent nucleopeptide-based hydrogels allow to develop complex supramolecular hydrogels driven by intermolecular interactions. But precise adjustment of the nucleopeptide sequences to modulate macroscopic properties requires a deep understanding at the atomic level of the intermolecular interactions occurring in the hydrogel. In particular, it is crucial to understand how solvent molecules interact with the nucleopeptide-based hydrogel fibres. Nuclear Magnetic Resonance is a well-known spectroscopic technique to obtain information at the atomic scale without altering the sample. NMR has already been used to characterize soft matter materials such as hydrogels and organogels[10]. High Resolution NMR can be used to unveil the presence of mobile nucleopeptides in the isotropic phase[10].

Hydrogels and organogels are mainly composed of solvent molecules (generally from > 95% to > 99.9% w/w). Fast Field Cycling NMR (FFC-NMR) relaxometry can be used to probe the dynamical behavior of the solvent inside of the gel[5,6,11]. FFC-NMR has proven its efficiency in the dynamical study of porous media. Kruk *et al.* worked on developing a model[12] to investigate water mobility in various matrixes such as hyaluronic dermal fillers[13], food[14,15] but also nanoparticles[16] in dextran-based hydrogels and other porous media as SiO_2 matrix filled with ionic liquids[17]. Tritt-Goc *et al.* also used FFC-NMR[18] to study supramolecular hydrogels[19] and organogels[20–22]. Bodart *et al.*[23]. were able to explain the water dynamics in

polygalacturonate hydrogels thanks to low field NMR relaxometry along with molecular dynamics simulations. They deciphered the adsorption/desorption phenomenon and the surface movements that were theorized by Stapf *et al.*[24,25]. Canet *et al.* also worked on gels, investigating the water and organic solvent behavior of different types of assemblies such as low-molecular-weight organogels with NMR relaxation and diffusion experiments[26,27] and hybrid silica gels to unveil the presence of two hydration layers[28]. Another approach was developed by Faux *et al.* for porous materials[29] and the study of relaxation rates of molecules in confined small pores[30]: the 3-Tau model[31]. This model is efficient to assess the dynamical behavior of water protons interacting with a solid interface[23,32]. The 3-Tau model comes with a user-friendly interface and brings various information about the water dynamics of the water inside the hydrogel sample. It also yields structural information by considering planar pore geometry for the hydrogel lattice where layer water can interact with the fibres. The 3-Tau model suits hydrogel study by providing insights into water dynamics and confinement within the gel structure. The efficiency of this model was already assessed by Bodart et al.[23] with the study of two polygalacturonate-based hydrogels, which are paramagnetic-free hydrogels as well as the nucleopeptide-based hydrogel of the present work. Thus, FFC NMR is a perfectly suitable tool to investigate nucleopeptide-based hydrogels and can be used, along with High Resolution NMR, to probe the complex gelation process that drives the nucleopeptides transition from their isotropic form to a network building a stable and stiff hydrogel.

This study aims to investigate the water dynamics within the gel matrix as well as the gelation process and its kinetics. The NMRD profiles provide insights into the different water pools and their mobility inside the hydrogel. By combining high-field NMR with low-field relaxometry, it becomes possible to unravel the kinetic pathway of hydrogel formation. Specifically, High-Resolution NMR is employed to probe nucleopeptide aggregation, while fixed low-field relaxometry focuses on water equilibration within the gel network. Furthermore, the temperature-dependent variations observed were exploited to propose mechanistic hypotheses underlying the transition toward the hydrogel state.

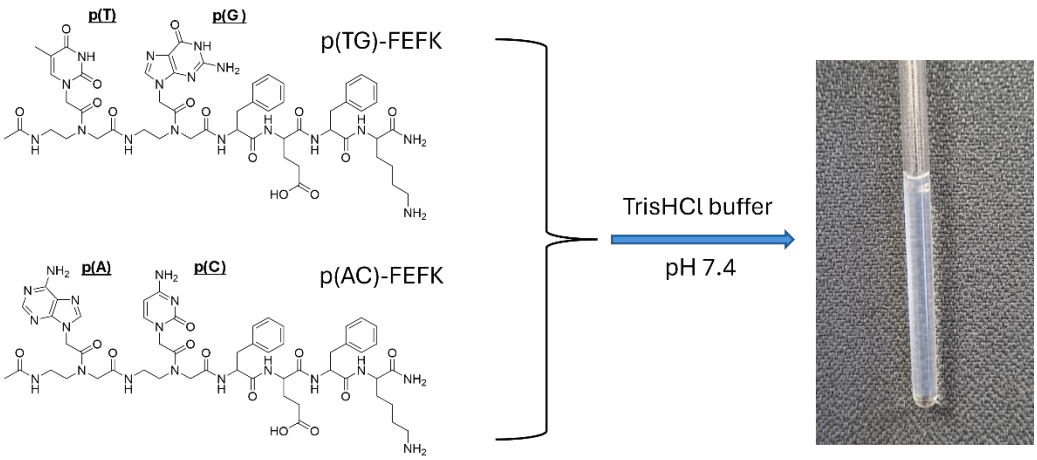

Figure 1 Nucleopeptides used for the hydrogel preparation, molecules are mixed in equimolar proportion for a total concentration of 15 mM.

2. MATERIALS AND METHODS

Sample preparation

Nucleopeptides were synthetized according to procedures described previously[8]. The hydrogel sample was prepared with equimolar nucleopeptides mixture (see Figure 1) for a global gelator concentration of 15 mM in a 1M TrisHCl buffer solution at pH 7.4 in deionized H_2O (18.2 MΩ.cm). It was then conditioned in two different NMR tubes, a 5 mm o.d. NMR tube for High-Resolution measurements (Figure 1) and, for sensitivity reasons, in a 10 mm o.d. NMR tube for FFC Relaxometry experiments.

FFC NMR measurements

FFC Relaxometry measurements were carried out on a Stelar SMARTracer fast-field-cycling relaxometer. NMRD profiles were acquired between 5 kHz and 3.75 MHz (^{1}H Larmor frequency) with 28 static field values sampled and a detection field of 7.2 MHz. Pre-polarized measurement sequence was used with a polarization duration of 1.5 s at 8 MHz. Field switching time was set at 3 ms with an 8 MHz/ms ramp. For each B_0, longitudinal relaxation rates R_1 were obtained from the magnetization monoexponential evolution as a function of time and sampled with 16 values from 0.01 to 4 times the longitudinal relaxation time. NMRD profiles were fitted with the 3-TM software using a spin surface density of 20 spins/nm^3[31]. Fixed field measurements for gelation kinetic study were acquired at 0.035 MHz using the pre-polarized sequence with the same parameters as the NMRD profiles.

High Resolution NMR experiments

High resolution NMR experiments were conducted on a Bruker Avance III spectrometer operating at 9.4 Tesla (400 MHz ^{1}H Larmor frequency) equipped with a 5 mm BBO probe, except for the gelation at 313 K where a 5 mm TBI probe was used. Temperature was varied from 293 K to 343 K with increments of 5 K. ^{1}H NMR spectra were acquired after a waiting time of 7 hours to stabilize the sample temperature. Water suppression was achieved using the NOESY-presaturation pulse sequence (Bruker 1D noesygppr1d pulse sequence) with irradiation at the water frequency during the recycle and mixing time delays. 256 scans with 4 dummy scans and a recycle delay of 15 s were used to follow the ^{1}H NMR spectra as a function of temperature; and 512 scans with 4 dummy scans and a recycle delay of 2 s were used to follow the gel formation (gelation kinetics) at 295 K and 313 K. Spectra processing including phasing, baseline correction and integrals measurements were performed on TopSpin 4.1 software.

3. RESULTS

Temperature effect on the nucleopeptide hydrogel

Tracking gelator molecules with High Resolution NMR. The effect of temperature on a gelified sample was investigated between 293 K and 343 K, using 5 K increments. Although the system remains visually fully gelified over this temperature range, signals from the gelator can still be detected in the ^{1}H NMR spectrum obtained at 9.4 T with water signal suppression (Figure 2). This indicates that a fraction of the gelator molecules does not participate in the gel network and remains sufficiently dynamic to be observed in solution.

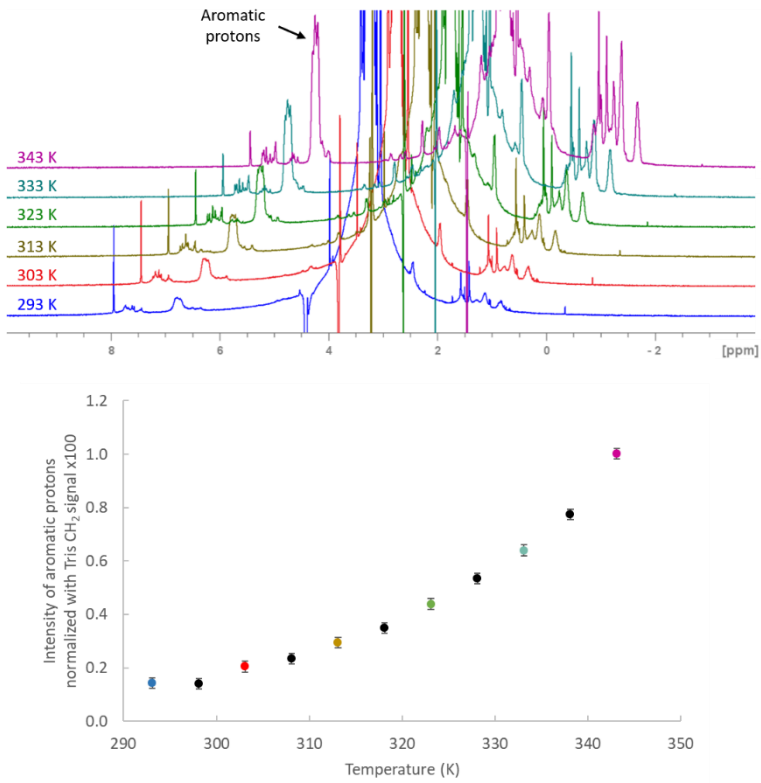

Figure 2 ^{1}H solution spectra of the hydrogel as a function of temperature (top) and normalized aromatic protons intensities (bottom) obtained from the different spectra. Gel concentration = 15 mM in TrisHCl pH 7.4.

A delay of 7 hours after each temperature adjustment ensured proper equilibration. All gelator signals follow the same trend; the aromatic protons of phenylalanine moieties (6.6–6.9 ppm) were chosen for quantification of the free gelator molecules. Their integral was normalized to the CH_2 signal of the TrisHCl buffer (3.23 ppm) to correct for possible spectrometer instabilities. Figure 2 summarizes the data obtained upon heating. No plateau was observed at high temperatures, confirming that the sample remains gelified even at 343 K, which was also verified visually. Since the sol–gel transition of this sample is expected near 353 K, further measurements with a high-temperature SEI probe will be performed to determine whether a plateau appears once all gelator aggregates are fully dissolved and observable in liquid-state NMR.

Water dynamics from FFC relaxometry. Water dynamical behavior was investigated at 295 K and 313 K thanks to Fast Field Cycling NMRD profiles (Figure 3).

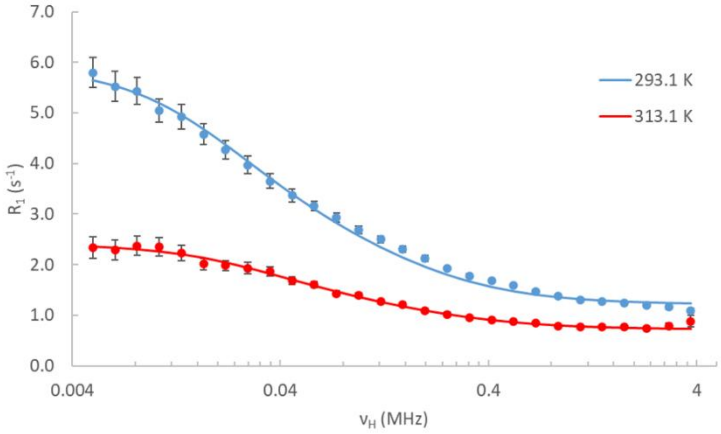

Figure 3 NMRD profiles of water protons in hydrogel at 295 K (blue) and 313 K (red). Gel concentration = 15 mM in TrisHCl pH 7.4.

Temperature clearly has an effect on water dynamics, particularly visible on the longitudinal relaxation of water protons at low field. The 3-Tau model was used through the 3TM software[33] to gather dynamical information via three correlation times: τ_b corresponding to bulk water, τ_l to the water layer molecules interacting with the fibres, and τ_d to the exchange rate between both pools. The model also provides a structural information in the form of a planar pore equivalent thickness h. This h value comes from the ratio between the surface layer thickness and the surface-to-volume ratio. The optimized parameters obtained with this model are summarized in Table 1.

Table 1 - 3-Tau fitting results of the hydrogel NMRD profiles curves at 295 K and 313 K.

temperature (K)	τ_l (µs)	τ_d (µs)	τ_b (ps)	h (nm)
295	0.65	2.05	13.3	136
313	0.49	1.33	7.5	267

As expected, all correlation times tend to decrease at higher temperature due to higher thermal agitation. Nevertheless, the τ_d/τ_l ratio, which gives the average number of hops of surface layer molecule prior to desorption[29,31], does not significantly change, meaning that the water-surface interactions strength is not strongly affected within the studied temperature range. The consistency of this ratio confirms that the fibers surface and their interaction with the water molecules are not altered by any chemical reaction. The equivalent pore size increases when

temperature increases, going from 136 nm at 295 K to 267 nm at 313K. Although in the same magnitude order of the previously reported values of the ovoidal pores dimension of 400-600 nm x 900-1200 nm for freeze-dried samples analyzed by cryoTEM[8], the values obtained by NMRD are smaller. Such differences can be due both to the quasi-two-dimensional pores approximation of the 3-tau model and the high heterogeneity of the hydrogel scaffold and the effect of freeze-drying on the sample. The apparent increase of pore size with temperature could correspond to an increase in mobility along hydrogel fibrils. Nevertheless, no modification of translational diffusion coefficient of water could be measured as a function of temperature at 400 MHz, the measured coefficient remains in the order of the one of bulk water ($1.4x10^{-9}$ $m^2.s^{-1}$ at 295 K and $2.1x10^{-9}$ $m^2.s^{-1}$ at 313 K).

The results demonstrate that water molecules exhibit increased dynamic behavior at elevated temperatures, accompanied by a higher proportion of unbound gelator. To elucidate the physicochemical mechanisms underlying these differences, the gelation kinetics were subsequently monitored at both temperatures, 295 K and 313 K.

Gelation kinetics at 295 K

Kinetics monitoring from the gelator point of view. Because the gelator molecules incorporated into the hydrogel lattice lack sufficient mobility to be detected by liquid-state NMR, the observed decay of the gelator signal over time after formulation can be attributed to their aggregation, i.e., the process of gel formation. To recover the liquid state in which the gelator molecules are solubilized, the hydrogel sample was first liquefied. For this, the 5 mm NMR tube containing the sample was heated to 353 K in a water bath for 5 min, followed by 1 min in an ultrasonic bath. This cycle was repeated twice to ensure complete dissolution of the nucleopeptides. The tube was then rapidly transferred to the spectrometer, set at 295 K, and successive ^1H NMR spectra with water suppression were recorded over a period of 60 h following hydrogel liquefaction.

Results are presented in Figure 4. The intensity of aromatic protons of phenylalanine, normalized to the CH_2 signal of the TrisHCl buffer, is represented as a function of time after liquefaction. All other signals of the gelator follow the same trend: an exponential decrease with a time constant of 3 h.

Water behavior during gelation. The hydrogel investigated is composed of 99 wt% solvent, meaning that water dominates its composition and thus serves as an excellent probe to indirectly

explore the gelation process. Because the behavior of water molecules is highly sensitive to their surrounding environment, monitoring their dynamics can provide valuable insights into structural changes occurring during gel formation. First, high-field relaxometry and diffusometry experiments were conducted to detect potential modifications in water mobility as gelation progressed. These measurements, however, revealed no significant alterations, suggesting that any changes in dynamics were too subtle or occurred on timescales inaccessible to these techniques. To overcome this limitation, low-field relaxometry was applied, as it is particularly sensitive to slower molecular motions. The longitudinal relaxation rate (R_1) of water was measured at a fixed ^{1}H frequency of 0.035 MHz over a period of 60 hours after liquefaction. As shown in Figure 3, R_1 at this frequency is a sensitive indicator of changes in water dynamics, with acquisition times short enough to resolve the kinetics of gel formation. The same liquefaction protocol as in the high-resolution experiments was used here. The resulting data are displayed in Figure 4.

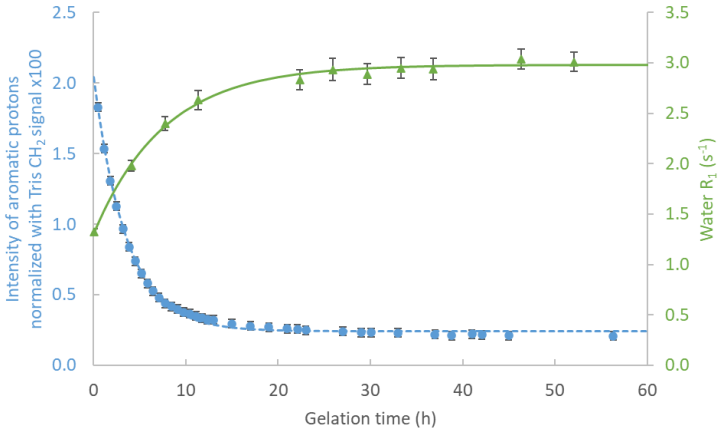

Figure 4 Aromatic protons signal decay (at 400 MHz ^{1}H Larmor frequency) as a function of time after liquefaction (blue) compared to the water R_1 evolution (measured at 0.035 MHz ^{1}H Larmor frequency) after liquefaction (green). Gel concentration = 15 mM in TrisHCl pH 7.4, T = 295 K.

Water R_1 increases with time, showing the impact of the gelation on water dynamics on the µs-ns timescale. Data were modelled with an exponential law that gives a time constant of 8 hours, surprisingly twice longer than the time constant obtained from the gelator point of view. High Resolution NMR and FFC Relaxometry unveiled two distinct time constants characterizing the gelation process: gelator signal decays with a short time constant of 3 h, whereas an 8 h time constant fits water R_1 evolution. Since High Resolution NMR focuses on the mobile gelator species (monomers and/or small aggregated objects), it highlights the early steps of the gelation process. Water R_1 study on the other hand features the global water equilibration inside the gelator 3D matrix, leading to the fully equilibrated hydrogel. As kinetics

of both phenomena bear different time constants, the building of the 3D network and subsequent water equilibration within this network are not concomitant.

Gelation kinetics at 313 K

Gelation kinetics were also studied at 313 K, using the same protocol as previously described: High Resolution NMR intensities of gelator molecules and low-field longitudinal relaxation of water.

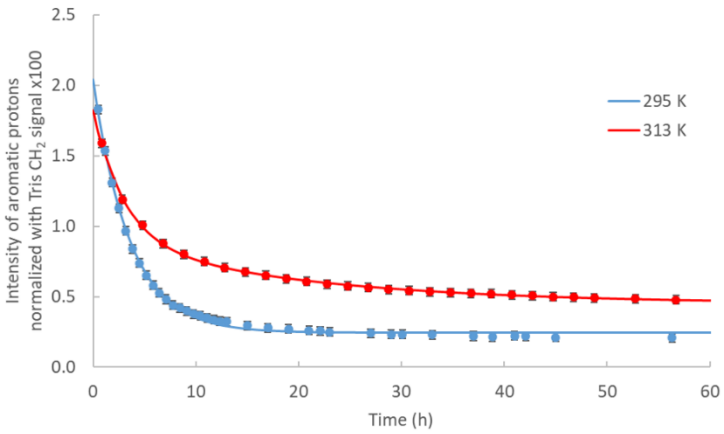

Figure 5 Normalized aromatic protons signal decay as a function of time after liquefaction of the hydrogel at 295 K (blue) and 313 K (red). Gel concentration = 15 mM in TrisHCl pH 7.4.

The gelation process, as seen from the gelator signal decay, takes longer at higher temperatures, as shown in Figure 5. This behavior may be related to the greater amount of free gelator molecules present at elevated temperatures (Figure 2). Interestingly, fitting the intensity profiles as a function of time requires a bi-exponential model with two characteristic time constants, 3 h and 20 h.

As shown in Figure 6, the evolution of water R_1 at 0.035 MHz over time is also slower at higher temperature, yielding a characteristic time constant of 20 h. Again, low-field relaxation measurements and direct observation of the gelator molecules provide distinct information. However, the time constant derived from R_1 is equal to one of those obtained from the gelator intensity kinetics at 313 K.

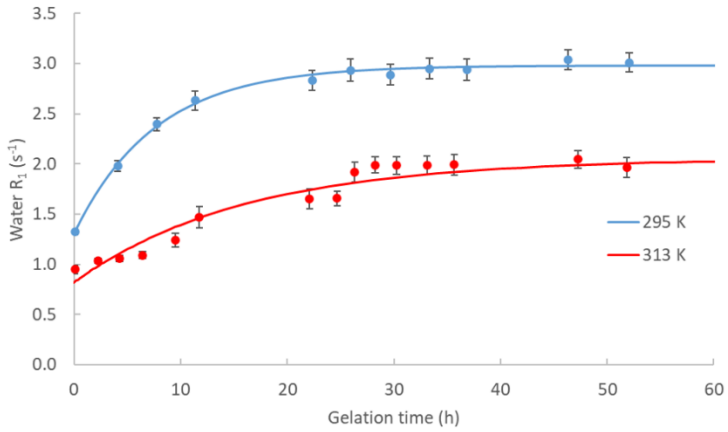

Figure 6 Water R_1 (0.035 MHz Larmor frequency) evolution as a function of time after liquefaction of the hydrogel at 295 K (blue) and 313 K (red).

Careful re-examination of the high-resolution data at 295 K indicates that, although a bi-exponential fit can be applied, it is not strictly required. The extracted time constants are 3 h and 8 h; however, the contribution of the longer component is minimal compared to that observed at 313 K.

These measurements demonstrate that gelation proceeds on two distinct timescales: a faster process (~3 h) and a slower one (approximately 8 h at 295 K and 20 h at 313 K). The existence of these two characteristic timescales is clearly evidenced by combining high-resolution measurements, which monitor the gelator molecules, with low-field longitudinal relaxation, which probes the water dynamics. This dual behavior may point to different underlying processes, such as an initial network formation followed by slower structural rearrangements or stabilization.

4. DISCUSSION

In light of these results, it is possible to make a hypothesis on this complex gelation process. At the early stages of the process, the nucleopeptides are fully dissolved and the monomers begin to aggregate. A longer time is then needed to enable these initial molecular structures to interact with each other, further aggregate and form the final hydrogel network that traps the water molecules, making the system undergo its transition from solution to gel state. Such results are consistent with the mesoscopic scale study made by Hoschtettler *et al.*[8]. Indeed, fluorescence experiments with thioflavin T (ThT) highlighted the presence of a first growth phase with t ≈ 2.5 h that corresponds to the initial formation of the fibers preceding a second

step where the fibrillar network becomes denser. They also observed two transitions in the ThT kinetic curves with an early aggregation process and metastable oligomers formation followed by the thermodynamically more stable structuration of the hydrogel. Nucleobases are also supposed to assemble before the peptide moieties.

Taking into account previous mesoscopic observations, our NMR results and the chemical nature of the nucleopeptides, one can hypothesize a gelation mechanism triggered by canonical pairing between the nucleobases. The second step corresponding to the global structuration of the hydrogel lattice, is probably driven by other interactions, possibly on the peptide side. We highlight that only the second stage of the global structuration is significantly affected by temperature variations, while the gel can still form and remain thermodynamically stable. At the same time, a higher proportion of free gelator molecules is observed at elevated temperatures. It can be assumed that gel formation therefore relies on two types of interactions: a strong, temperature-independent interaction that sustains the gel structure below the gel–sol transition, and a weaker, temperature-sensitive interaction. The latter might be associated with hydrogen bonding in the peptide segment, particularly involving residues with greater conformational flexibility and higher susceptibility to thermal agitation.

5. CONCLUSION

Thanks to Fast Field Cycling NMR Relaxometry combined with High-Resolution NMR, we were able to investigate the gelation process and its kinetics. By looking both at gelator signal quantity (HR NMR) and water dynamics (FFC NMR) along the gelation time, we were able to formulate a strong hypothesis on a multi-step gelation process for this nucleopeptide-based hydrogel. Even if monomers aggregate and agglomerate quickly, a longer time is needed to form the whole 3-dimensional network fully equilibrated with water, leading to the thermodynamically stable gelified state. Given the previous mesoscopic-scale study, the nucleobases pairing could govern the first early aggregation phenomenon, whereas peptide interactions could occur predominantly during the following equilibration step. The temperature dependence of the gelation process was also studied with the same methodology and unveiled that only the second step of the gelation process is strongly impacted by the temperature rise; its kinetic time doubles because of the longer fibrillar structuration of the gel network. The temperature effect on a macroscopically gelified sample was investigated between 293 K and 343 K. No plateau was reached within this temperature range, confirming the maintaining of the gelified state even at 343 K. Future studies will include further measurements

at higher temperatures since the sol-gel transition is expected to be near 353 K. Finally, NMRD profiles have proven to be useful to probe the water dynamics inside the hydrogel matrix at both temperatures, showing quicker correlation times at higher temperature. Such a technique will be used to investigate the kinetics at low field by acquiring several NMRD profiles along the gelation process and by looking at the evolution of the derived correlation times. A more detailed analysis of the mechanisms governing such complex assemblies will be performed by solid-state NMR as part of an upcoming work.

Acknowledgements

The authors would like to thank the CPM NMR facility of Université de Lorraine for access to High Resolution spectrometers. L.S. and P.H. thank the Agence Nationale de la Recherche (ANR-20-CE06-0010-01 MUNCH) for funding. G.C. thanks the ORION program for its contribution to the funding of her research internship (government grant managed by the Agence Nationale de la Recherche with the reference ANR-20-SFRI-0009).

References

[1] A. Saiani, A. Mohammed, H. Frielinghaus, R. Collins, N. Hodson, C. M. Kielty, M. J. Sherratt, A. F. Miller, "Self-assembly and gelation properties of α-helix versus β-sheet forming peptides" *Soft Matter* **2008**, *5*, 193–202, 10.1039/B811288F.

[2] J. Wychowaniec, Designing Nanostructured Peptide Hydrogels Containing Graphene Oxide and Its Derivatives for Tissue Engineering and Biomedical Applications, **2018**.

[3] J. K. Wychowaniec, A. M. Smith, C. Ligorio, O. O. Mykhaylyk, A. F. Miller, A. Saiani, "Role of Sheet-Edge Interactions in β-sheet Self-Assembling Peptide Hydrogels" *Biomacromolecules* **2020**, *21*, 2285–2297, 10.1021/acs.biomac.0c00229.

[4] M. I. A. Ibrahim, J. Bodiguel, G. Pickaert, L. Stefan, K. Matsuo, M.-C. Averlant-Petit, "Supramolecular hydrogels derived from 2 : 1-[α/aza]-pseudopeptides: design, structural analysis and self-assembly in solution, solid, and gel states" *J. Mater. Chem. B* **2025**, *13*, 7437–7448, 10.1039/d4tb02288b.

[5] T. Giraud, S. Bouguet-Bonnet, P. Marchal, G. Pickaert, M.-C. Averlant-Petit, L. Stefan, "Improving and fine-tuning the properties of peptide-based hydrogels *via* incorporation of peptide nucleic acids" *Nanoscale* **2020**, *12*, 19905–19917, 10.1039/D0NR03483E.

[6] T. Giraud, S. Bouguet-Bonnet, M.-J. Stébé, L. Richaudeau, G. Pickaert, M.-C. Averlant-Petit, L. Stefan, "Co-assembly and multicomponent hydrogel formation upon mixing nucleobase-containing peptides" *Nanoscale* **2021**, *13*, 10566–10578, 10.1039/D1NR02417E.

[7] T. Giraud, P. Hoschtettler, G. Pickaert, M.-C. Averlant-Petit, L. Stefan, "Emerging low-molecular weight nucleopeptide-based hydrogels: state of the art, applications, challenges and perspectives" *Nanoscale* **2022**, *14*, 4908–4921, 10.1039/D1NR06131C.

[8] P. Hoschtettler, G. Pickaert, A. Carvalho, M.-C. Averlant-Petit, L. Stefan, "Highly Synergistic Properties of Multicomponent Hydrogels Thanks to Cooperative Nucleopeptide Assemblies" *Chem. Mater.* **2023**, *35*, 4259–4275, 10.1021/acs.chemmater.3c00308.

[9] P. L. Scognamiglio, C. Vicidomini, G. N. Roviello, "Dancing with Nucleobases: Unveiling the Self-Assembly Properties of DNA and RNA Base-Containing Molecules for Gel Formation" *Gels* **2023**, *10*, 16, 10.3390/gels10010016.
[10] Y. E. Shapiro, "Structure and dynamics of hydrogels and organogels: An NMR spectroscopy approach" *Progress in Polymer Science* **2011**, *36*, 1184–1253, 10.1016/j.progpolymsci.2011.04.002.
[11] S. Bouguet-Bonnet, T. Giraud, L. Stefan, M.-C. Averlant-Petit, D. Canet, "On the Observation of ^{14}N Quadrupole Resonance Transitions in Water Proton NMR Relaxometry Dispersion Curves: The Case of a Labile NH Grouping in a Semirigid Molecular Moiety" *J. Phys. Chem. B* **2022**, *126*, 7159–7165, 10.1021/acs.jpcb.2c05208.
[12] D. Kruk, *Understanding Spin Dynamics*, Jenny Stanford Publishing, **2015**.
[13] D. Kruk, P. Rochowski, E. Masiewicz, S. Wilczynski, M. Wojciechowski, L. M. Broche, D. J. Lurie, "Mechanism of Water Dynamics in Hyaluronic Dermal Fillers Revealed by Nuclear Magnetic Resonance Relaxometry" *ChemPhysChem* **2019**, *20*, 2816–2822, 10.1002/cphc.201900761.
[14] D. Kruk, M. Florek – Wojciechowska, E. Masiewicz, M. Oztop, A. Ploch-Jankowska, P. Duda, S. Wilczynski, "Water mobility in cheese by means of Nuclear Magnetic Resonance relaxometry" *Journal of Food Engineering* **2021**, *298*, 110483, 10.1016/j.jfoodeng.2021.110483.
[15] P. Pocan, E. Ilhan, M. Florek–Wojciechowska, E. Masiewicz, D. Kruk, M. H. Oztop, "Exploring the water mobility in gelatin based soft candies by means of Fast Field Cycling (FFC) Nuclear Magnetic Resonance relaxometry" *Journal of Food Engineering* **2021**, *294*, 110422, 10.1016/j.jfoodeng.2020.110422.
[16] E. Umut, M. J. Beira, M. H. Oztop, N. Sahiner, P. J. Sebastião, D. Kruk, "Water Dynamics in Dextran-Based Hydrogel Micro/Nanoparticles Studied by NMR Diffusometry and Relaxometry" *J. Phys. Chem. B* **2023**, *127*, 8950–8960, 10.1021/acs.jpcb.3c04452.
[17] D. Kruk, M. Wojciechowski, S. Brym, R. K. Singh, "Dynamics of ionic liquids in bulk and in confinement by means of 1H NMR relaxometry – BMIM-OcSO4 in an SiO2 matrix as an example" *Phys. Chem. Chem. Phys.* **2016**, *18*, 23184–23194, 10.1039/C6CP02377K.
[18] J. Tritt-Goc, A. Rachocki, M. Bielejewski, "The solvent dynamics at pore surfaces in molecular gels studied by field-cycling magnetic resonance relaxometry" *Soft Matter* **2014**, *10*, 7810–7818, 10.1039/C4SM01140F.
[19] J. Kowalczuk, A. Rachocki, M. Bielejewski, J. Tritt-Goc, "Effect of gel matrix confinement on the solvent dynamics in supramolecular gels" *Journal of Colloid and Interface Science* **2016**, *472*, 60–68, 10.1016/j.jcis.2016.03.033.
[20] M. Bielejewski, J. Tritt-Goc, "Evidence of Solvent−Gelator Interaction in Sugar-Based Organogel Studied by Field-Cycling NMR Relaxometry" *Langmuir* **2010**, *26*, 17459–17464, 10.1021/la103324s.
[21] J. Tritt-Goc, M. Bielejewski, R. Luboradzki, "Interaction of chlorobenzene with gelator in methyl-4,6-O-(p-nitrobenzylidene)-α-d-glucopyranoside gel probed by proton fast field cycling NMR relaxometry" *Tetrahedron* **2011**, *67*, 8170–8176, 10.1016/j.tet.2011.08.040.
[22] J. Kowalczuk, M. Bielejewski, A. Łapiński, R. Luboradzki, J. Tritt-Goc, "The Solvent–Gelator Interaction as the Origin of Different Diffusivity Behavior of Diols in Gels Formed with Sugar-Based Low-Molecular-Mass Gelator" *J. Phys. Chem. B* **2014**, *118*, 4005–4015, 10.1021/jp412511e.
[23] P. R. Bodart, P. Fouilloux, A. Rachocki, A. Lerbret, T. Karbowiak, A. Assifaoui, "Slow water dynamics in polygalacturonate hydrogels revealed by NMR relaxometry and

molecular dynamics simulation" *Carbohydrate Polymers* **2022**, *298*, 120093, 10.1016/j.carbpol.2022.120093.
[24] S. Stapf, R. Kimmich, R.-O. Seitter, "Proton and Deuteron Field-Cycling NMR Relaxometry of Liquids in Porous Glasses: Evidence for L\'evy-Walk Statistics" *Phys. Rev. Lett.* **1995**, *75*, 2855–2858, 10.1103/PhysRevLett.75.2855.
[25] S. Stapf, R. Kimmich, R.-O. Seitter, "Field-cycling NMR relaxometry of liquids confined in porous glass: Evidence for levy-walks" *Magnetic Resonance Imaging* **1996**, *14*, 841–846, 10.1016/S0730-725X(96)00213-5.
[26] S. Bouguet-Bonnet, M. Yemloul, D. Canet, "New Application of Proton Nuclear Spin Relaxation Unraveling the Intermolecular Structural Features of Low-Molecular-Weight Organogel Fibers" *J. Am. Chem. Soc.* **2012**, *134*, 10621–10627, 10.1021/ja303679z.
[27] M. Yemloul, E. Steiner, A. Robert, S. Bouguet-Bonnet, F. Allix, B. Jamart-Grégoire, D. Canet, "Solvent Dynamical Behavior in an Organogel Phase As Studied by NMR Relaxation and Diffusion Experiments" *J. Phys. Chem. B* **2011**, *115*, 2511–2517, 10.1021/jp200281f.
[28] D. Oulkadi, M. Yemloul, S. Desobry-Banon, D. Canet, "Water behavior in hybrid silica gels as studied by 1H nuclear magnetic resonance relaxometry. Evidence of two hydration layers" *Microporous and Mesoporous Materials* **2013**, *172*, 213–216, 10.1016/j.micromeso.2013.01.030.
[29] D. Faux, R. Kogon, V. Bortolotti, P. McDonald, "Advances in the Interpretation of Frequency-Dependent Nuclear Magnetic Resonance Measurements from Porous Material" *Molecules* **2019**, *24*, 3688, 10.3390/molecules24203688.
[30] D. A. Faux, P. J. McDonald, "Explicit calculation of nuclear-magnetic-resonance relaxation rates in small pores to elucidate molecular-scale fluid dynamics" *Phys. Rev. E* **2017**, *95*, 033117, 10.1103/PhysRevE.95.033117.
[31] R. Kogon, D. Faux, A. Assifaoui, P. Bodart, "Advanced insight on the water dynamics of anisotropic hydrogels by field-cycling nuclear magnetic resonance: Application of 3-Tau model" *Carbohydrate Polymers* **2023**, *314*, 120922, 10.1016/j.carbpol.2023.120922.
[32] D. A. Faux, P. J. McDonald, N. C. Howlett, "Nuclear-magnetic-resonance relaxation due to the translational diffusion of fluid confined to quasi-two-dimensional pores" *Phys. Rev. E* **2017**, *95*, 033116, 10.1103/PhysRevE.95.033116.
[33] R. Kogon, D. Faux, "3TM: Software for the 3-Tau Model" *SoftwareX* **2022**, *17*, 100979, 10.1016/j.softx.2022.100979.